

Comparison of picosecond electron dynamics in isolated and clustered Si quantum dots deposited on a semiconductor surface

Keiki Fukumoto,^{1, a)} Ayse Seyhan,^{2, b)} Ken Onda,³ Shunri Oda,⁴ and Shin-ya Koshihara⁴

¹⁾*High Energy Accelerator Research Organization (KEK), 1-1 Oho, Tsukuba, Ibaraki 305-0801 Japan*

²⁾*Omer Halisdemir University, Nanotechnology Application and Research Center, 51240 Niğde, Turkey*

³⁾*Kyushu University, 744 Motoooka, Nishi-ku, Fukuoka 819-0395, Japan*

⁴⁾*Tokyo Institute of Technology, 2-12-1 Ookayama, Meguro-ku, Tokyo 152-8550, Japan*

(Dated: 10 July 2019)

Semiconductor quantum dots (QDs) have been widely used in various optoelectronic devices. Extensive studies have been devoted to the application of Si QDs with the aim of realizing various optoelectronic functions based on the modified energy band structure in QDs compared with bulk crystals. Therefore, it is necessary to be able to directly probe the carrier dynamics in single Si QDs of nanoscale dimensions deposited on a SiO₂/Si surface, where the environment is compatible with Si-based semiconductor devices. This letter reports the observation and comparison of the ultrafast electron dynamics just after the photoexcitation of isolated and clustered Si QDs on a SiO₂/Si surface using time-resolved photoemission electron microscopy with spatial and temporal resolutions of 50 nm and 100 fs, respectively. The detailed structure of QDs was confirmed directly by scanning electron microscopy observations. The results obtained in the present study show that the carrier lifetime in isolated QDs is shorter than that in clustered QDs. This is consistent with the electron-hole interaction in nano-space significantly modifying the carrier recombination rates.

PACS numbers: 61.46.+w, 72.20.Jv, 73.63.-b, 79.60.-i

Keywords: Quantum dots, Electron dynamics, Imaging

^{a)}keiki@post.kek.jp

^{b)}aseyhan@ohu.edu.tr

Semiconductor quantum dots (QDs) offer functionality beyond that of Si by controlling electron transport properties as a result of quantum confinement^{1–12}. The most attractive optoelectronic property of Si-based QDs is their ability to emit light. Room-temperature photoluminescence (PL) was first observed in porous Si¹³ and later in QDs^{2,10,14,15}. Growth techniques for Si QDs narrowing their size distribution and controlling the dot density (distance between neighboring QDs)^{16,17}, have contributed to the exploration of the properties of QDs. However, it should be noted that these properties have been probed in bulk form, i.e., by averaging the data collected from a number of QDs mostly in a solvent^{9,18,19}. Recently, time dependent photoluminescence from single dots, which were fabricated by top-down technique based on lithography and oxidization processes, has been successfully detected on the timescale of nanoseconds¹¹. However, there have been very few studies on the picosecond carrier dynamics of Si QDs deposited on an oxidized Si surface an environment compatible with Si devices. One of reasons for this is that individual QDs are structurally different from each other at the nanoscale and thus they each independently contribute to the carrier dynamics. On the femtosecond to picosecond timescales, dynamics are not only energy relaxation of photogenerated carriers and band gap recombination, but also surface recombination because of the large surface-to-volume ratio^{9,18–21} and carrier multiplication (CM) by one photon absorption^{8,22–24}. This is also another reason to investigate intrinsic dynamics of QDs intricate.

The band gap of QDs can be controlled by controlling the dot size when the quantum confinement effect appears, at which point the valence and conduction bands (VB and CB) are split^{25–27}. When the energy gap between the bands exceeds the thermal energy, carrier transitions between them are suppressed, resulting in the lengthening of the hot carrier lifetime; this is called the phonon bottleneck²⁸. However, fast relaxation on the order of picoseconds against it has been observed due to the confinement effect in QDs^{29–31}. A shorter relaxation time in smaller QDs (stronger electron–hole interactions) has been reported for compound semiconductors^{4,5,32,33} and Si^{7,8,34}.

The present article reports the direct observation and comparison of the dynamics of photogenerated carriers in the picosecond regime for isolated and clustered Si QDs ($\phi = 10$ nm) deposited on a SiO₂/Si surface. The dynamics of photogenerated electrons in identical QDs were investigated by time-resolved photoemission electron microscopy (TR-PEEM) using femtosecond laser pulses (see for example^{35,36}), and the nano-scale structures of isolated or clustered QDs were identified by scanning electron microscopy (SEM) observations. The relaxation time in QD clusters

was found to be longer than that in isolated QDs. Carriers in the clusters were more spatially separated than in single QDs, which resulted a longer relaxation time, as theoretically expected and experimentally observed for larger QDs. It was demonstrated that the nanostructure influences the ultrafast carrier dynamics in Si QDs deposited on a solid surface.

Si QDs were fabricated on a SiO₂/Si substrate via decomposition of SiH₄ using a vibrational high-frequency (VHF, 144 MHz) plasma-enhanced chemical vapor deposition (CVD) system, which allows the grain size to be controlled via gas phase nucleation and growth of nanocrystals^{16,17}. Using a small slit (5 mm), Si QDs were extracted from the plasma cell and deposited on the substrate at room temperature in an ultrahigh-vacuum chamber. The base pressure and working pressure were below 10⁻⁹ Torr and 1 mTorr, respectively. A piezoelectric valve was used to provide a pulsed silane (SiH₄, 1.4 sccm) supply, and Ar gas was supplied continuously to the plasma cell at a flow rate of 90 sccm. To form Si QDs with a uniform size, pulsed SiH₄ gas was introduced into the plasma cell with on and off times of 0.1 and 1.0 s, respectively. After deposition of QDs, samples were transferred to the TR-PEEM ultrahigh vacuum chamber in the air so that the surfaces of Si QDs were covered with a few layers of natural oxide.

The structure of the Si QD samples was studied using field emission scanning electron microscopy (FE-SEM; Hitachi S-5000). Figure 1(a) shows a typical SEM image of a measured sample in this study. Si QDs can be observed as individual or clustered white droplets and were found to be well isolated by distances on the order of tens of nanometers. The dot density and size were controlled via the plasma power and gas flow rate. The density of Si QDs was estimated to be approximately 2.5/(100 nm)² based on a number of SEM images, including Figure 1(a). Si QDs were also deposited onto a SiN₂ membrane in the same manner for transmission electron microscopy (TEM; JEOL JEM-2012F) observations in order to estimate the size distribution. Typical TEM images are shown in Figures 1(b) and 1(c). TEM observations confirmed that the Si QDs were single crystals with high crystallinity and that they were spherical. The mean size of the Si QDs was 10 nm, as shown in Figure 1(d).

An overview of the TR-PEEM experiments and the observed dynamics is shown in Figure 2. Figure 2(a) is an SEM image of a sample with dimensions of 1 μm × 2 μm formed from eight merged images, where Si QDs appear with greater contrast and a rounded shape. To reduce surface contamination and image deterioration, the scan rate of the electron beam was increased, and the spatial resolution was reduced to the minimum value at which QDs could be distinguished as isolated or clustered.

The green, orange, and red $60 \text{ nm} \times 60 \text{ nm}$ boxes shown in Figure 2(a) are areas that include no QDs, isolated QDs, and clustered QDs, respectively. Using a spatial resolution of 50 nm for the present setup of the TR-PEEM system enabled the selective observation of photogenerated electron lifetimes in each of these square areas. The details of this technique can be found in previous papers^{35,37–39}. The energy of pump pulse is 2.4 eV , which is larger than the band gap of the QDs (approximately 1.2 eV for $\phi \approx 10 \text{ nm}$)²⁶. However, in order to excite electrons at Γ points, the fluence was optimized to induce two photon process and to observe electron dynamics (Fig. 4). The pump pulse on the sample surface was elliptical with dimensions of $10 \mu\text{m} \times 20 \mu\text{m}$. The photon density was set to excite 0.1 electrons in a single QD per pulse. After photoexcitation by the pump pulse, the time-dependence of the photogenerated electron density (lifetime) was monitored by the amount of photoemission induced by the probe pulse ($h\nu = 4.8 \text{ eV}$). The size of the probe pulses on the sample surface was approximately 10 times larger than that of the generated pump pulse. A temporal resolution of approximately 100 fs was estimated from the full width at half maximum (FWHM) of the cross correlation of the pump and probe pulses, which was 240 fs .

TR-PEEM images were obtained at different pump–probe delay times Δt ranging from -1.8 ps to 4.2 ps at intervals of 0.1 ps . Four examples of clipped TR-PEEM images with the same area as the image in Figure 2(a) at $\Delta t = -1, 0, 0.2,$ and 1 ps are shown on the right-hand side of the figure. To obtain each image at different delay times Δt , photoemission signals emitted by 3,000,000 probe pulses were accumulated. Photoexcitation can be recognized from the enhancement of the photoemission intensity at 0 ps in comparison with the image obtained at a negative delay.

Figure 2(b) shows the photoemission intensity averaged over the whole area plotted against Δt . Numerical fitting with the convolution of $A_0 + A\exp(-\Delta t/\tau)$ and a Gaussian function with $2\sigma = 240 \text{ fs}$ yielded a decay constant τ of 0.7 ps . To obtain the electron dynamics in the green, orange, and red boxes in Figure 2(a), the spatial correlation of the SEM and PEEM images was confirmed with a nanoscale resolution. The detailed procedure for this can be found in the Supplementary Information. Figures 2(c)–(e) show the time dependence of the photoemission intensity averaged over the areas with no QDs, isolated QDs, and clustered QDs, respectively. For the areas with isolated and clustered QDs (Figures 2(d) and 2(e)), the estimated decay constants τ were 0.5 and 1.1 ps , respectively, and no dynamic event was observed in the areas with no QDs (Figure 2(c)). Note that the square areas used to analyze these three cases were selected such that pixel noise in the TR-PEEM images and the printed text in the SEM image were avoided. Figure 3 shows five randomly selected and enlarged images from each the three types of regions in the SEM image

(Figure 2(a)). These images confirm that the proper forms of the Si QDs were selected.

This section discusses the origin of the observed electron dynamics. To date, three types of electron dynamics in Si QDs on a picosecond timescale have been reported: energy relaxation in the CB, surface recombination to the VB, and carrier multiplication (CM) by interband^{8,22–24} and intraband^{40–42} transitions in QDs. However, the efficiency of CM was negligibly small in the present experimental setup. Because the surface dynamics is dominant in Si QDs with a surface oxide layer, and also the energy of the pump pulse is only twice that of the band gap of Si QDs (1.2 eV) with a diameter of 10 nm^{3,22,43–45}. Ultrafast electron dynamics has been observed also in bulk Si. Sjodin *et al.* reported that the sub-ps electron transfer from L valley to X valley, in which a sample was a Si wafer covered with a native oxide surface layer. They measured intrinsic bulk properties by reflectivity of 400 nm-laser pulses, which is less sensitive to the dynamics with surface properties⁴⁶. Therefore, we propose a model for the electron dynamics in Si QDs with a three-level rate equation consisting of energy relaxation and recombination to the VB via the surface states^{2,9,18,19} (Figure 4). The three levels are denoted as the excited state (ES), the surface states (SS), and the VB maximum (VBM), and the time-dependent electron densities for each state are denoted by $N_{ES}(t)$, $N_{SS}(t)$, and $N_{VBM}(t)$, respectively. The relaxation and surface recombination time constants are denoted by τ_1 and τ_2 , respectively. The initial conditions are $N_{ES}(t) = N$ and $N_{SS}(t) = N_{VBM}(t) = 0$. Because τ_2 is size-independent¹⁸, it was fixed to the faster decay time constant of 0.5 ps obtained from the fitting in Figure 2(d). Furthermore, τ_1 is size-dependent because of the confinement effect^{4,5,19,32,33}. The probe pulses ($h\nu = 4.8$ eV) induced photoemission from the CB and SS but not from the VB; therefore, the photoemission intensity detected using this experimental setup was $N_{ES}(t) + N_{SS}(t)$ (Figure 4).

Figures 5(a) and 5(b) show the observed electron dynamics in the isolated and clustered QDs shown in Figures 2(d) and 2(e), respectively. The black curves in Figures 5(a) and 5(b) are the results of numerically fitting the experimental data with a convolution of $N_{ES}(t) + N_{SS}(t)$ and the pulse correlation function with $2\sigma = 240$ fs. Figures 5(c) and 5(d) show $N_{ES}(t)$ and $N_{SS}(t)$ for isolated and clustered QDs, respectively, along with the correlation function. The time constant τ_1 obtained by numerical fitting the data for the isolated and clustered QDs is given in Figures 5(a) and 5(b), respectively. The results indicate that electron–hole interactions in isolated QDs are stronger than those in clusters, as illustrated at the top of Figure 5, resulting in a lower τ_1 of 0.1 ps in isolated QDs than that of 0.7 ps in clusters. These timescales are of the same order of magnitude as the size-dependent relaxation time in CdSe QDs⁵. These results indicate that clusters behave

like larger QDs.

In summary, the relaxation and recombination dynamics of photogenerated electrons in Si QDs with diameters of 10 nm deposited on a SiO₂/Si surface, where the environment is compatible with Si-based devices, were investigated using TR-PEEM with high spatial and temporal resolutions of 50 nm and 100 fs, respectively. TR-PEEM enabled the observation of the carrier dynamics of each well-isolated QD, and SEM observations in the same area provided more detailed structural information, such as whether the QDs were isolated or clustered. The behavior of clustered QDs is similar to that of larger QDs, which exhibit a longer relaxation time than isolated QDs as a result of their weaker electron–hole interactions.

SUPPLEMENTARY MATERIAL

See the supplementary material for the details of the way to evaluate spatial correlation of SEM and PEEM images, and for the dynamics in a small number of quantum dots.

ACKNOWLEDGMENTS

This work was supported financially by JST CREST, JSPS KAKENHI Grant No.JP15K17677 and JSPS KAKENHI for Scientific Research on Innovative Areas 'Soft Crystals' (Area No. 2903, No.JP17H06366), Japan.

REFERENCES

- ¹F. Priolo, T. Gregorkiewicz, M. Galli, and T. F. Krauss, *Nature Nanotechnology* **9**, 19 (2014).
- ²W. D. A. M. de Boer, D. Timmerman, K. Dohnalova, I. N. Yassievich, H. Zhang, W. J. Buma, and T. Gregorkiewicz, *Nature Nanotechnology* , 878 (2010).
- ³G. Nair, L.-Y. Chang, S. M. Geyer, and M. G. Bawendi, *Nano Letters* **11**, 2145 (2011).
- ⁴V. I. Klimov and D. W. McBranch, *Phys. Rev. Lett.* **80**, 4028 (1998).
- ⁵V. I. Klimov, D. W. McBranch, C. A. Leatherdale, and M. G. Bawendi, *Phys. Rev. B* **60**, 13740 (1999).
- ⁶P. Sippel, W. Albrecht, D. Mitoraj, T. Eichberger, R. Hannappel, and D. Vanmaekelbergh, *Nano letters* **13**, 1655 (2013).

- ⁷Y. R. Bergren, C. E. Kendrick, N. R. Neale, J. M. Redwing, R. T. Collins, T. E. Furtak, and M. C. Beard, *J. Phys. Chem. Lett.* **5**, 2050 (2014).
- ⁸M. C. Beard, K. P. Knutsen, P. Yu, J. M. Luther, Q. Song, W. K. Metzger, R. J. Ellingson, and A. J. Nozik, *Nano Letters* **7**, 2506 (2007).
- ⁹F. Trojanek, K. Neudert, P. Maly, K. Dohnalova, and I. Pelant, *J. Appl. Phys.* , 116108 (2006).
- ¹⁰C. Delerue, G. Allan, C. Reynaud, O. Guillois, G. Ledoux, and F. Huisken, *Phys. Rev. B* **73**, 235318 (2006).
- ¹¹I. Sychugov, J. Valenta, and J. Linnros, *Nanotechnology* **28**, 072002 (2017).
- ¹²F. Pevere, I. Sychugov, F. Sangghaleh, A. Fucikova, and J. Linnros, *Journal of Physical Chemistry C* **119**, 7499 (2015).
- ¹³M. V. Wolkin, J. Jorne, P. M. Fauchet, G. Allan, and C. Delerue, *Phys. Rev. Lett.* **82**, 197 (1999).
- ¹⁴L. Tsybeskov, J. V. Vandyshev, and P. M. Fauchet, *Phys. Rev. B* **49**, 7821 (1994).
- ¹⁵L. Van Dao, X. Wen, M. T. T. Do, P. Hannaford, E.-C. Cho, Y. H. Cho, and Y. Huang, *J. Appl. Phys.* **97**, 013501 (2005).
- ¹⁶T. Ifuku, M. Otobe, A. Itoh, and S. Oda, *Jpn. J. Appl. Phys.* **36**, 4031 (1997).
- ¹⁷K. Nishiguchi, X. Zhao, and S. Oda, *J. Appl. Phys.* **92**, 2748 (2002).
- ¹⁸V. I. Klimov, C. J. Schwarz, D. W. McBranch, and C. W. White, *Appl. Phys. Lett.* , 2603 (1998).
- ¹⁹D. G. Cooke, A. N. MacDonald, A. Hryciw, J. Wang, Q. Li, A. Meldrum, and F. A. Hegmann, *Phys. Rev. B* **73**, 193311 (2006).
- ²⁰T. Schmidt, A. I. Chizhik, A. M. Chizhik, K. Potrick, A. J. Meixner, and F. Huisken, *Phys. Rev. B* **86**, 125302 (2012).
- ²¹S. Kim, D. H. Shin, and S.-H. Choi, *Appl. Phys. Lett.* **100**, 253103 (2012).
- ²²G. Nair, S. M. Geyer, L.-Y. Chang, and M. G. Bawendi, *Phys. Rev. B* **78**, 125325 (2008).
- ²³R. D. Schaller, J. M. Pietryga, and V. I. Klimov, *Nano Letters* **7**, 3469 (2007).
- ²⁴G. Nair and M. G. Bawendi, *Phys. Rev. B* **76**, 081304 (2007).
- ²⁵Y. M. Niquet, C. Delerue, G. Allan, and M. Lannoo, *Phys. Rev. B* **62**, 5109 (2000).
- ²⁶M. Mahdouani, R. Bourguiga, S. Jaziri, S. Gardelis, and A. G. Nassiopoulou, *Phys. Stat. Sol. a* **205**, 2630 (2008).
- ²⁷H.-C. Weissker, J. Furthmüller, and F. Bechstedt, *Phys. Rev. B* **65**, 155327 (2002).
- ²⁸A. Nozik, *Annu. Rev. Phys. Chem.* **52**, 193 (2001).
- ²⁹A. L. Efros, V. A. Kharchenko, and M. Rosen, *Solid State Communications* **93**, 281 (1995).
- ³⁰S. V. Kilina, D. S. Kilin, and O. V. Pprezhdo, *ACS Nano* **3**, 93 (2009).

- ³¹R. D. Schaller, J. M. Pietryga, S. V. Goupalov, M. A. Petruska, S. A. Ivanov, and V. I. Klimov, *Phys. Rev. Lett.* **95**, 196401 (2005).
- ³²J. M. Harbold, H. Du, T. D. Krauss, K.-S. Cho, C. B. Murray, and F. W. Wise, *Phys. Rev. B* **72**, 195312 (2005).
- ³³R. R. Cooney, S. L. Sewall, K. E. H. Anderson, E. A. Dias, and P. Kambhampati, *Phys. Rev. Lett.* **98**, 177403 (2007).
- ³⁴M. Sykora, L. Mangolini, R. D. Schaller, U. Kortshagen, D. Jurbergs, and V. I. Klimov, *Phys. Rev. Lett.* **100**, 067401 (2008).
- ³⁵K. Fukumoto, Y. Yamada, K. Onda, and S.-y. Koshihara, *Appl. Phys. Lett.* **104**, 053117 (2014).
- ³⁶M. Dabrowski, Y. Dai, and H. Petek, *J. Phys. Chem. Lett.* **8**, 4446 (2017).
- ³⁷K. Fukumoto, K. Onda, Y. Yamada, T. Matsuki, T. Mukuta, S.-i. Tanaka, and S.-y. Koshihara, *Rev. Sci. Instrum.* **85**, 083705 (2014).
- ³⁸K. Fukumoto, Y. Yamada, S. Koshihara, and K. Onda, *Appl. Phys. Exp.* **8**, 101201 (2015).
- ³⁹K. Fukumoto, Y. Yamada, T. Matsuki, K. Onda, T. Noguchi, R. Mizokuchi, S. Oda, and S. Koshihara, *Proc. 19th International conference on Ultrafast Phenomena* **162**, 337 (2015).
- ⁴⁰M. T. Trinh, R. Limpens, W. D. A. M. de Boer, J. M. Schins, L. D. A. Siebbeles, and T. Gregorkiewicz, *Nature Photonics* **6**, 316 (2012).
- ⁴¹D. Timmerman, I. Izeddin, P. Stallinga, I. N. Yassievich, and T. Gregorkiewicz, *Nature Photonics* **2**, 105 (2008).
- ⁴²A. Takeuchi, T. Kuroda, K. Mase, Y. Nakata, and N. Yokoyama, *Phys. Rev. B* **62**, 1568 (2000).
- ⁴³J. E. Murphy, M. C. Beard, A. G. Norman, S. P. Ahrenkiel, J. C. Johnson, P. Yu, O. I. Mičić, R. J. Ellingson, and A. J. Nozik, *J. Am. Chem. Soc.* **128**, 3241 (2006).
- ⁴⁴R. J. Ellingson, M. C. Beard, J. C. Johnson, P. Yu, O. I. Micic, A. J. Nozik, A. Shabaev, and A. L. Efros, *Nano Letters* **5**, 865 (2005).
- ⁴⁵R. D. Schaller, M. A. Petruska, and V. I. Klimov, *Appl. Phys. Lett.* **87**, 253102 (2005).
- ⁴⁶T. Sjoedin, H. Petek, and H. Dai, *Phys. Rev. Lett.* **81**, 5664 (1998).

FIG. 1. (a) SEM and (b), (c) TEM images of Si QDs. The size distribution of the Si QDs was estimated from the TEM images to be approximately $\phi = 10$ nm. Si QDs are single crystals with a high degree of crystallinity.

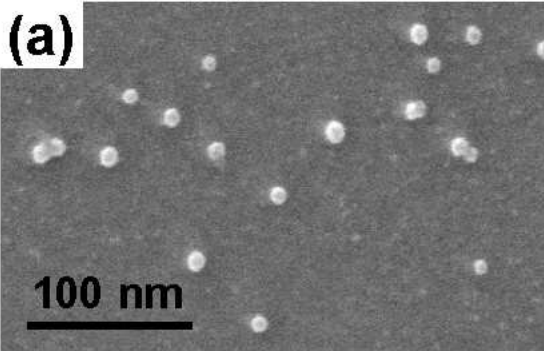
FIG. 2. Schematic illustration of TR-PEEM setup with four example TR-PEEM images taken at different pump-probe delay times of $-1, 0, 0.2,$ and 1 ps. (a) SEM image taken at $\Delta t = -1$ ps with green, orange, and red $60 \text{ nm} \times 60 \text{ nm}$ boxes indicating areas that include no QDs, isolated QDs, and clustered QDs, respectively. Time-dependent photoemission intensity PE_{int} for (b) the whole area in the SEM image, (c) areas without QDs, (d) areas with isolated QDs, and (e) areas with clusters. The black curves in (b)–(d) were obtained by numerically fitting the plots with $PE_{\text{int}} = A_0 \times A \exp(-\Delta t / \tau)$.

FIG. 3. Enlarged views of randomly selected square regions from Figure 2(a) for each type of area: without QDs, with isolated QDs, and with clustered QDs. The dimensions of each box are $60 \text{ nm} \times 60 \text{ nm}$.

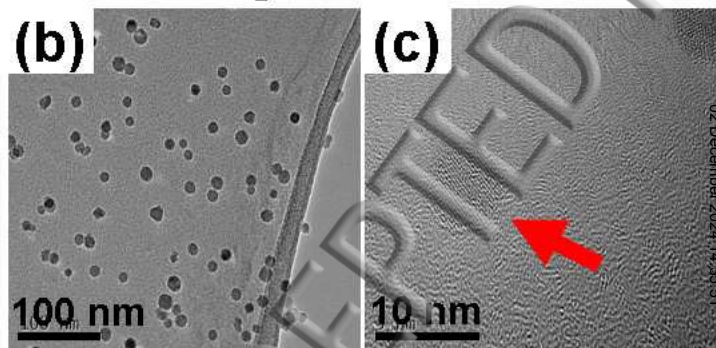
FIG. 4. Simplified Si band structure including the relaxation process for photogenerated electrons. $N_{ES}(t)$, $N_{SS}(t)$, and $N_{VBM}(t)$ are the time-dependent electron densities in the ES, SS, and VBM, respectively. τ_1 and τ_2 are the decay constants from ES to SS and SS to VBM, respectively.

FIG. 5. (a), (b) Fitting results from Figures 2(d) and 2(e). (c), (d) Temporal changes in N_{ES} and N_{SS} plotted with the correlation function, which has an FWHM of 240 fs.

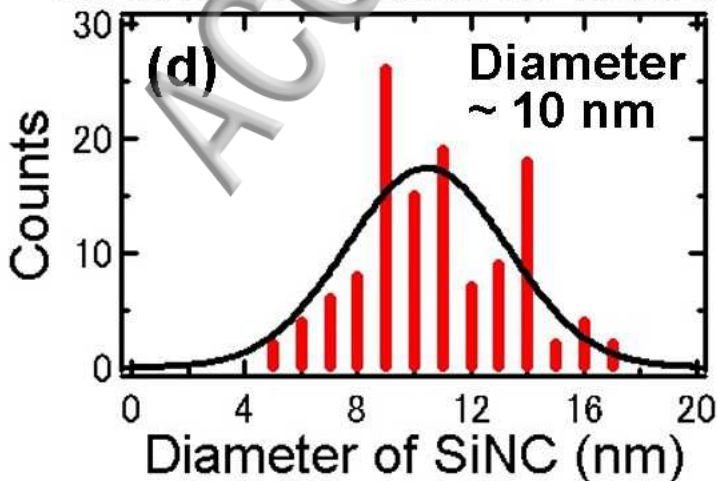
SEM images of SiQDs



TEM images of SiQDs



Size distribution of SiQDs



Pump pulse
2.4 eV
 $\phi = 10 \mu\text{m}$

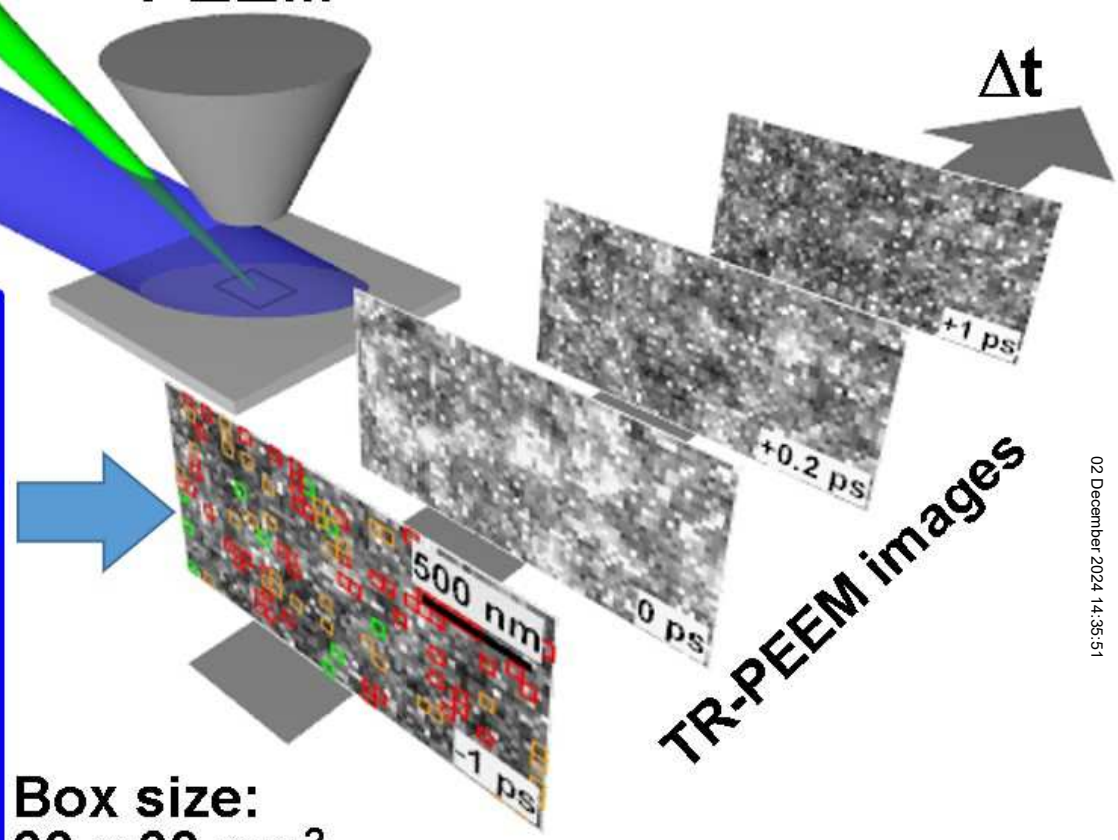
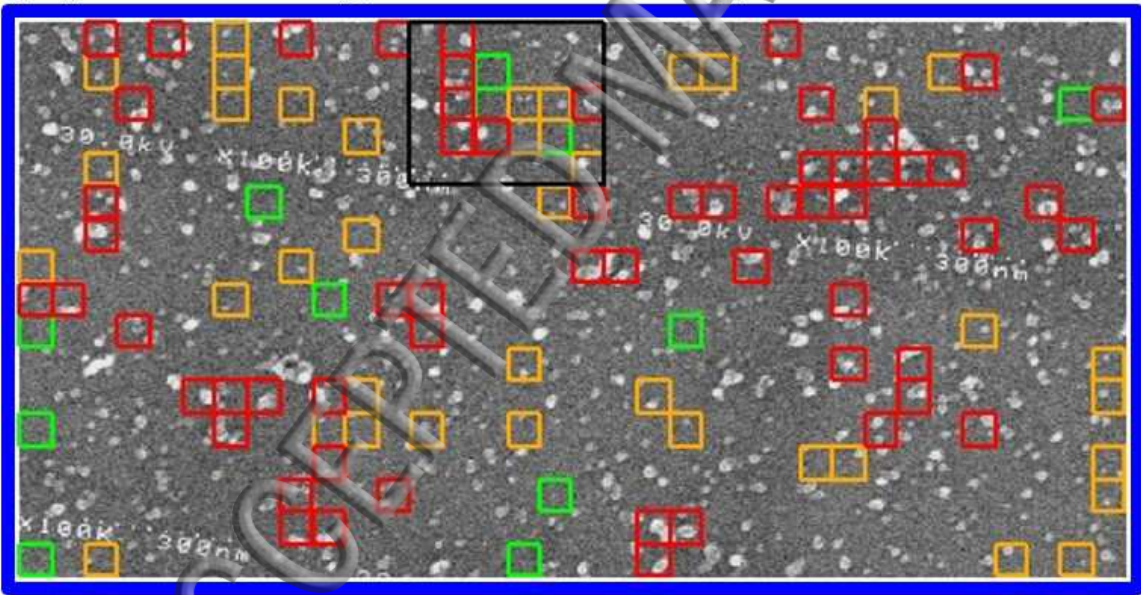
Probe pulse
4.8 eV
 $\phi = 1 \text{mm}$

Δt

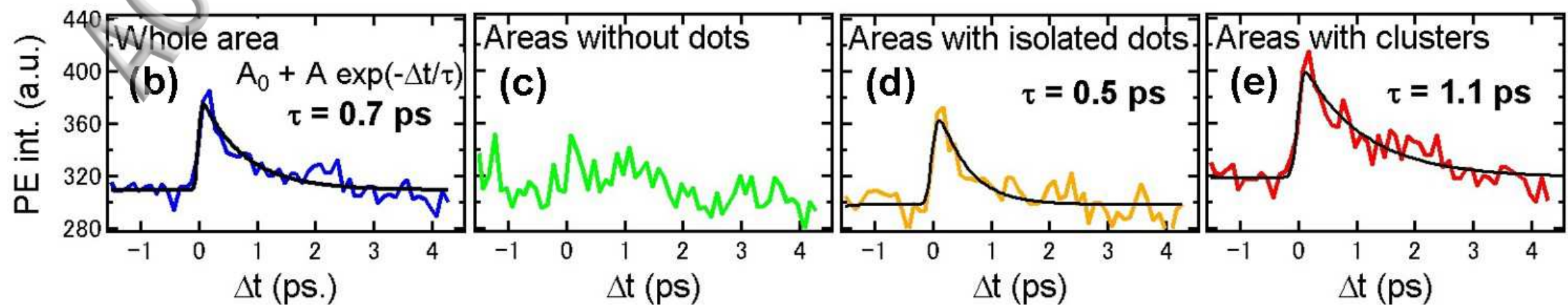
PEEM

Δt

(a) SEM image: SiQDs/SiO₂/Si



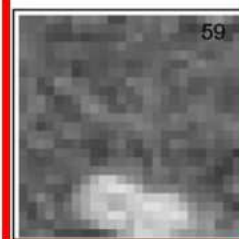
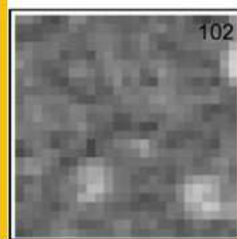
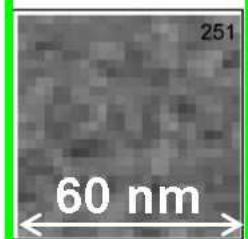
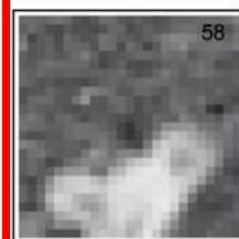
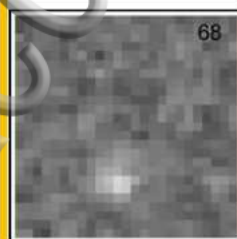
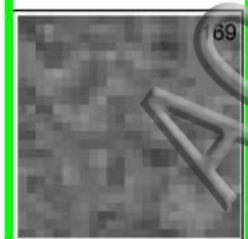
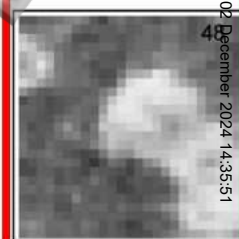
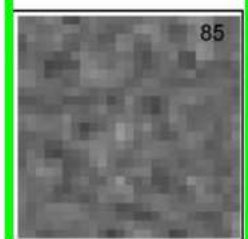
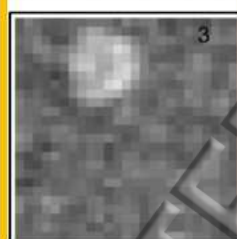
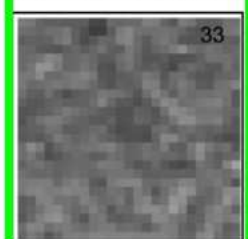
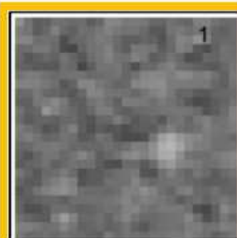
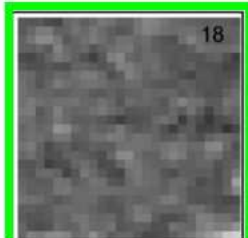
Box size:
60 x 60 nm²



without dots

isolated dots

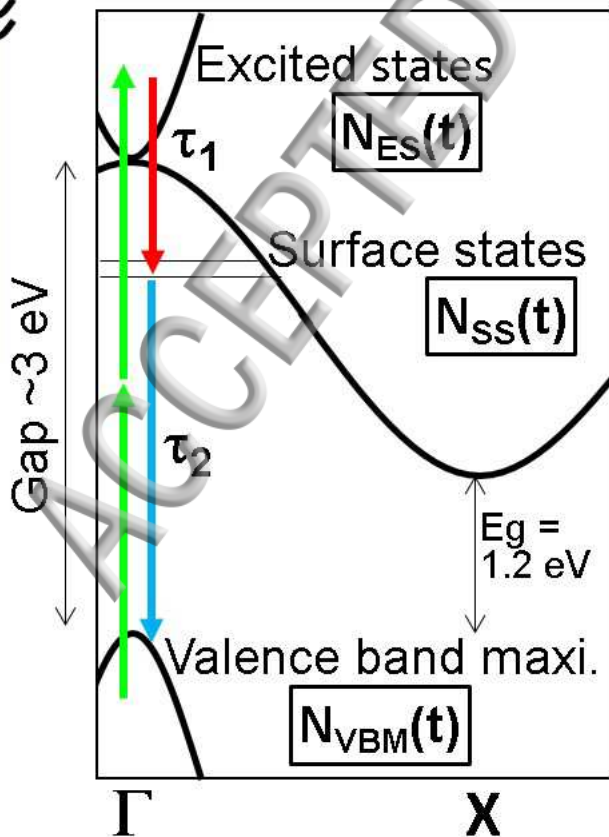
clusters



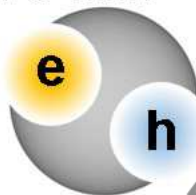
02 December 2024 14:35:51

$N_{ES}(t) + N_{SS}(t)$

Photoemission by
probe pulses (4.8 eV)



Isolated QDs
 $\phi = 10$ nm



Clustered QDs

